GESEP – Gerência de Especialistas em Sistemas Elétricos de Potência

Título:

COMPARISON OF HARMONIC DETECTION METHODS APPLIED IN A PHOTOVOLTAIC INVERTER DURING HARMONIC CURRENT COMPENSATION

Autores:

F. Antunes, L. S. Xavier, A. F. Cupertino, L. B. Felix e H. A. Pereira

Publicado em:

2017 Brazilian Power Electronics Conference (COBEP)

Data da Publicação:

2017

Citação para a versão publicada:

F. Antunes, L. S. Xavier, A. F. Cupertino, L. B. Felix and H. A. Pereira, "Comparison of harmonic detection methods applied in a photovoltaic inverter during harmonic current compensation," 2017 Brazilian Power Electronics Conference (COBEP), Juiz de Fora, 2017, pp. 1-6.

COMPARISON OF HARMONIC DETECTION METHODS APPLIED IN A PHOTOVOLTAIC INVERTER DURING HARMONIC CURRENT COMPENSATION

Felipe Antunes[1], Lucas S. Xavier[3], Allan F. Cupertino[3,4], Leonardo B. Felix[2], Heverton A. Pereira[2]
[1]Graduate Program in Electrical Engineering UFSJ/CEFET – MG, Federal University of São João del-Rei,
São João del-Rei – MG, Brazil.
[2]Electrical Engineering Department, Federal University of Viçosa – UFV, Viçosa - MG, Brazil.
[3]Graduate Program in Electrical Engineering, Federal University of Minas Gerais, Belo Horizonte - MG, Brazil.
[4] Materials Engineering Department, Federal Center for Technological Education of Minas Gerais,
Belo Horizonte – MG, Brazil
e-mail: antunesfelipe.elt@gmail.com, lsantx@gmail.com, afcupertino@ieee.org, leobonato@ufv.br, heverton.pereira@ufv.br.

Abstract **– Traditional harmonic current detection methods track all harmonic contents of the load and the control tuning tends to be complex with low flexibility. However, several applications require a harmonic detector method able to track the higher load harmonic current. This work analysis three harmonic detector methods: Fast Fourier Transform (FFT), Iterative Discrete Fourier Transform (IDFT) and based on Second Order Generalized Integrator (SOGI-PLL) structure. All methods are applied in an adaptive current harmonic control strategy applied in multifunctional single-phase photovoltaic inverter. Simulation results show that the IDFT method is faster and more accurate in the harmonic detection than the SOGI-PLL based method. However, SOGI-PLL structure is more robust during grid voltage frequency fluctuation.**

Keywords − **Discrete Fourier transform, harmonic current detector, harmonic compensation, second order generalized integrator.**

I. INTRODUCTION

Nowadays the power system is experiencing an increase in the number of non-linear loads at all levels of supply. Harmonic components can increase the power-system losses, damage sensitive loads, cause excessive heating in rotating machinery, create interference in communication systems, generating noise in regulating devices and control systems [1].

The active power filter (APF) is considered a very promising approach to control harmonic pollution [2]. In APF, firstly, the harmonic current components of the load are detected, and secondly these currents are cancelled. Thus, the performance of the APF depends strongly on the detecting method. Several algorithms for harmonic analysis and frequency estimation have been proposed in the literature, based on Discrete Fourier Transform [3], [4], [5], Kalman filter [3], p-q Theory [3], Adaptive Notch Filter [1], Second order generalized integrator [6], Modulation-function integral observer [7], Wavelet [8], Neural Network [9], [10] and Fuzzy [11].

The detectors can be analyzed by several characteristics, such as, required measurements (VxI), response time, steady state accuracy, selective harmonic compensation, single and three-phase application, need for synchronous sampling,

computational consumption time, estimation of the dc offset, circularity of fundamental and inter-harmonics effects **[7]**.

In [6] was proposed a novel adaptive current harmonic control strategy applied in multifunctional single-phase photovoltaic inverters with proportional multi-resonant controller, which requires a harmonic detector capable of tracking the higher harmonic component. The detector proposed by [6] consists in a cascade association of two phase-locked loop based on second order generalized integrator (SOGI-PLL), this detector combines features that meet this application.

Other detectors can be applied to solve this problem, such as detectors based on the Discrete Fourier Transform (DFT). Differently of the SOGI-PLL, DFT method needs to estimate several harmonics, and then, compare one each other to determine which is the largest harmonic component.

This paper compares three harmonic detector methods: two based on DFT and one based on SOGI-PLL. All methods are applied in a single-phase photovoltaic inverter to harmonic current compensation.

This work is organized as follow. In Section II the harmonic current detections methods are described, and in Section III these methods are compared. In Section IV the case study and the preliminary results are described. Finally, conclusions are stated in Section V.

II. HARMONIC DETECTION METHODS

A. Discrete Fourier Transform (DFT)

Discrete Fourier Transform (DFT) is a mathematical transformation of discrete signals which gives both amplitude and phase information of the desired harmonic [12].

The DFT method requires the current measurement and can be applied in both single or in three phase systems. If the current is continuously sampled, the harmonic components can be obtained using the point by point window sliding DFT algorithm with the latest N-sampled current signal.

The DFT requires a coherent sampling, which refers to a certain relationship between grid frequency (f_{grid}), sampling frequency (F_s), number of cycles in the sampled signal (M_{cycle}) and number of samples (N), related by:

$$\frac{f_{grid}}{F_s} = \frac{M_{cycle}}{N}. \tag{1}$$

The sampling frequency (F_s) must be a multiple of the grid frequency (f_{grid}). This ensures that the information of the fundamental and harmonic components are contained within the DFT bins, avoiding spectral leakage.

The f_{grid} is a constant and N depends of the F_s and M_{cicle} chosen. For higher F_s larger memory and computational efforts are required to ensure a real-time application. On the other hand, lower F_s increases the problems with aliasing and decrease the range of harmonics that can be analyzed.

Higher M_{cycle} requires larger computational memory, and slower transient response. However, the detector is more robust in the presence of noise or inter-harmonics. For a faster DFT dynamic, normally $M_{cycle} = 1$ is chosen.

In a discrete-time current signal $i[n]$, the DFT is applied on the window of the last N-samples, defined as:

$$\dot{I}_h[n] = \sum_{k=1}^{N} i[k + n - N]e^{-j\frac{2\pi h}{N}k} = I_h e^{j\emptyset}, \quad (2)$$

where, $0 \le h \le N/2$ is the order of the harmonic, $\dot{I}_h[n]$ is the hth current harmonic complex expectral component, I_h and $\emptyset$ is the magnitude and the angle of the hth current harmonic, respectively.

Once the harmonics are detected and the higher harmonic is identified, it is just a matter of reconstruction back in time-domain to create the compensation signal for the controller:

$$i_{h_{max}}[n] = \frac{2}{N} Re\{I_{h_{max}} e^{j(\emptyset max)}\}. \quad (3)$$

A.1 Fast Fourier Transform (FFT)

The window sliding DFT can be performed with the Fast Fourier Transform (FFT) algorithm since the number of samples (N) is a regular power of 2. The FFT provides a whole spectrum and reduce the total number of calculations from N^2 to $N\log_2 N$ [12]. The scheme of the detector is shown in the Fig. 1.
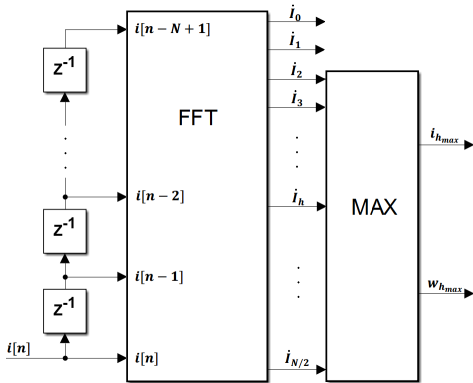
Fig. 1. DFT harmonic extraction scheme.

The FFT block receives the last N-samples and provide the whole spectrum to the MAX block, which is responsible for comparing the magnitude of all harmonics and return the signal of higher amplitude and your angular frequency.

A.2 Iterative Discrete Fourier Transform (IDFT)

Sliding window iterative discrete Fourier transform (IDFT) algorithm has been widely applied in real problems, due to its simple implementation and good real-time performance [13]. The main idea of sliding window iteration is using the latest real-time sampling data to detect the harmonic current, removing the first sampling data [5].

Every time that a new sample is added to the window the first sample of the old window is removed to keep the size fixed in N samples, as can be seen in Fig. 2:
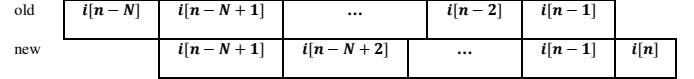
Fig. 2. Iterative discrete Fourier transform considering the addition of a new point.

The only differences between the old and the new window are the first and the last samples, but all the other samples are the same. The DFT equation for the old and the new window can be expressed as:

$$\dot{I}_h[n-1] = i[n-N]e^{-j\frac{2\pi h 1}{N}} + i[n-N+1]e^{-j\frac{2\pi h 2}{N}} + i[n-1]e^{-j\frac{2\pi h N}{N}}. \quad (4)$$

$$\dot{I}_h[n] = i[n-N+1]e^{-j\frac{2\pi h 1}{N}} + \cdots + i[n-1]e^{-j\frac{2\pi h (N-1)}{N}} + i[n]e^{-j\frac{2\pi h N}{N}}. \quad (5)$$

Thus,

$$\dot{I}_h[n] = e^{j\frac{2\pi h}{N}}\dot{I}_h[n-1] + i[n] - i[n-N]. \quad (6)$$

According to the Euler's formula, the above sliding DFT equation can be expanded as:

$$\dot{I}_h[n] = \left(cos\left(\frac{2\pi h}{N}\right) - jsin\left(\frac{2\pi h}{N}\right)\right)\left(Re(\dot{I}_h[n-1]) + jIm(\dot{I}_h[n-1]) + i[n] - i[n-N]\right). \quad (7)$$

Thus, the real and imaginary part of the spectrum point can be derived from (7) as:

$$Re(\dot{I}_h[n]) = Re(\dot{I}_h[n-1])cos\left(\frac{2\pi h}{N}\right) + Im(\dot{I}_h[n-1])sin\left(\frac{2\pi h}{N}\right) + i[n] - i[n-N]. \quad (8)$$

$$Im(\dot{I}_h[n]) = Im(\dot{I}_h[n-1])cos\left(\frac{2\pi h}{N}\right) - Re(\dot{I}_h[n-1])sin\left(\frac{2\pi h}{N}\right). \quad (9)$$

Equations (8) and (9) can be expressed by the structure shown in the Fig. 3.

The complete detector is shown in the Fig. 4. For each harmonic in the output there is one structure, as shown in Fig. 3, that provide the complex harmonic component to the MAX block.
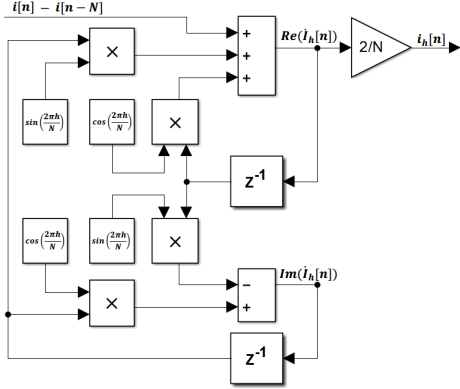
Fig. 3. Structure of the real sliding iterative DFT.

This method does not require reconstruction, once the harmonic current can be directly obtained, as show the Fig. 3. Additionally, this method has the advantage to allow selectable subset detection harmonic between the second and the N/2, for example, the lower odd harmonics set.
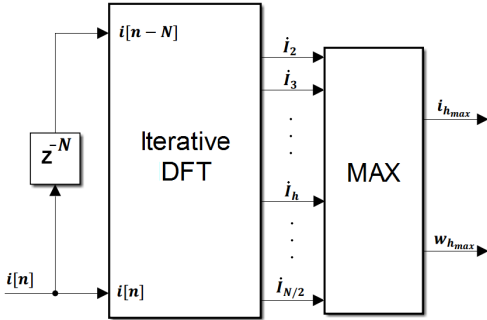
Fig. 4. Iterative DFT harmonic extraction scheme.

B. Harmonic Current Detector Based on SOGI-PLL

In this section, the single-phase representation of the harmonic current detection method based on SOGI-PLL is addressed. This current detector structure is shown in Fig. 5 (a) and it is based on a cascaded SOGI-PLL structure [14] [6], as represented in Fig. 5 (b). The idea of this method takes advantage of the interaction between the SOGI adaptive filter, whose its bandwidth only depends on the gain k [14] [15], and the SRF-PLL, whose its transfer function is given by [16]:

$$\frac{\theta_h(s)}{\theta_{in}(s)} = \frac{K_{p,pll}s + K_{i,pll}}{s^2 + K_{p,pll}s + K_{i,pll}}, \tag{10}$$

where θ_h and θ_{in} are the output and input phase angle, respectively. $K_{p,pll}$ and $K_{i,pll}$ are the PI controller gains. The expression shown in (10) is a standard second order transfer function. It is defined $K_{p,pll} = 2\zeta\omega_n$ and $K_{i,pll} = \omega_n^2$, where ζ is the damping factor and $\omega_n = 2\pi f_n$ is the SRF-PLL natural frequency [16].

The input current $i_L(t)$, as shown in Fig. 5, is a signal composed of all frequency components from the load current. The aim of the first stage is to detect the load fundamental current component $i_1(t)$. The SOGI-PLL structure of this stage extracts the amplitude I_1, frequency ω_1 and phase angle θ_1 informations of the fundamental component. Low-pass filters (LPF) in the amplitude and frequency detection are important to avoid the influence of the harmonic components

that the SOGI-PLL bandwidth can not suppress. This signal is reconstructed, represented by $i_1(t)$ and subtracted from the input current. The resulting signals are the harmonic components presented in the load current, as suggested by the following equation:

(a)

(b)
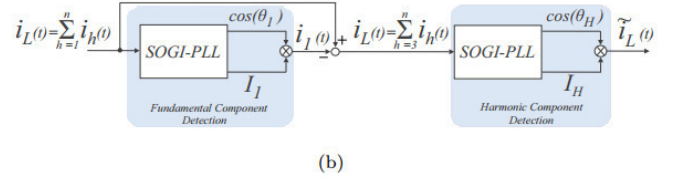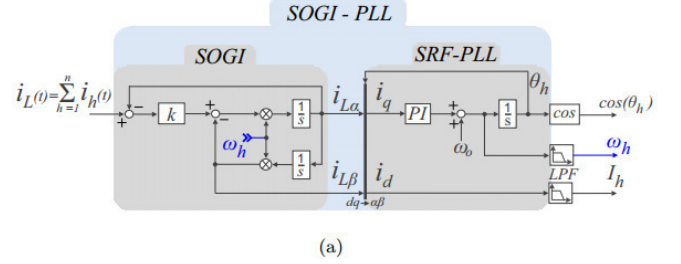
Fig. 5. (a) Current harmonic detection method based on SOGI-PLL. (b) General structure of SOGI-PLL.

$$i_L(t) = \sum_{h=2}^{n} i_h(t) \tag{11}$$

The second stage consists to detect the predominant harmonic component present in the load current (11). The amplitude, frequency and phase angle informations are extracted. The current signal is reconstructed $\tilde{i}_L(t)$ and sent to the control loop to perform the harmonic compensation of this predominant load harmonic current.

The frequency of the detected harmonic is used as feedback to tune the resonant controller. In this case, only two resonant controllers are needed, the first one controlling the fundamental current and the second one, controlling the predominant load harmonic current component [6].

III. STRATEGIES COMPARISON

In this section a comparison of the load harmonic current detection methods is done: the first one in the time domain strategy (SOGI-PLL) and the other two in frequency domain (DFT and IDFT). Both strategies are designed to detect the load harmonic current component of higher amplitude, making possible the selective harmonic compensation.

For this comparison, two disturbances are applied on the system. The first one is a change in the load current harmonic content. The second one is a frequency fluctuation, in the range of 1Hz in the fundamental frequency. The current spectra of the loads used in this study are shown in Fig. 6. The load 1 has a 5th harmonic component of 10A, a 7th harmonic component of 5A and a 11th harmonic component of 3A. The load 2 has a 5th harmonic component of 3A, a 7th harmonic component of 10A and a 11th harmonic component of 5A. In the load 2 and 3, the harmonic components are multiples of 60Hz. The load 3 has the same harmonic amplitudes of the load 2 but its harmonic components are multiples of 61Hz.
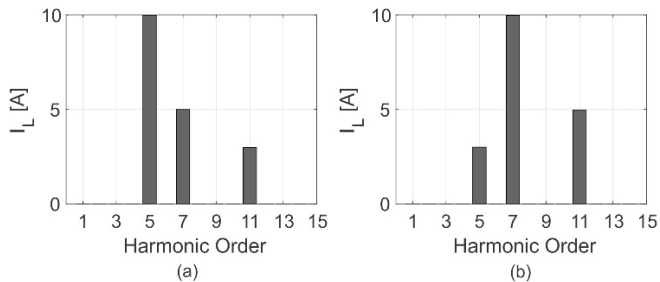
Fig. 6. Current spectra of the loads (a) load 1 (b) load 2 and load 3.

In Fig. 7 is shown the beginner of the detection process. In this time, the 5th harmonic component of the load 1 is detected by both methods. Note that the DFT and IDFT have a faster response than the SOGI-PLL based method for tracking the 5th harmonic component. In five cycles of 300 Hz, the DFT detects the 5th harmonic current component. The SOGI-PLL based method leads fifty cycles of 300Hz for tracking the same current.
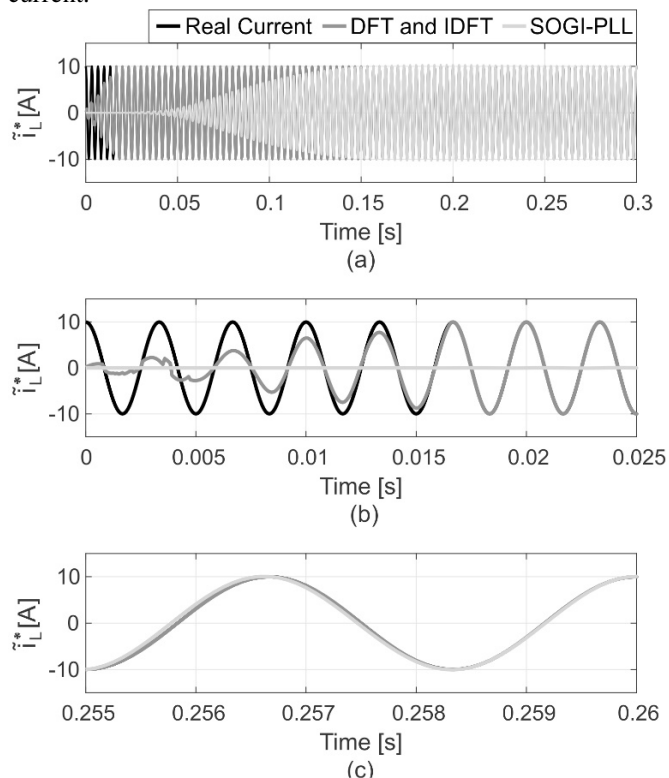
Fig. 7. The 5th harmonic component detection of the load 1. (a) General overview. (b) Transient response. (c) Steady state response.

This can be explained because there are three stages in the SOGI-PLL and each one is responsible to detect each harmonic component of the load current. For this reason, the stages are turned on cascading. Additionally there are the own dynamics of each stage. In steady state, the two strategies have a similar performance with a slight delay in the SOGI-PLL based method signal. It is possible to observe that the DFT and IDFT have an identical performance with higher detection accuracy.

In Fig. 8 is shown the 7th harmonic component detection of the load 2 using all methods. Again, the DFT has a faster response than the SOGI-PLL based method for tracking this

harmonic. In steady state, the two strategies have a similar performance with a slight delay in the SOGI-PLL based.
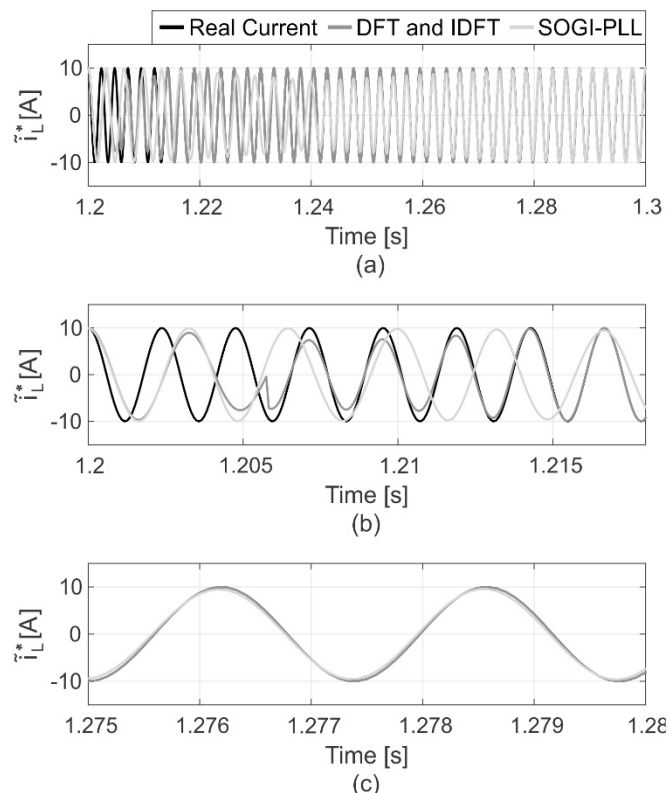
Fig. 8. The 7th harmonic component detection of the load 2. (a) General overview. (b) Transient response. (c) Steady state response.

In Fig. 9 is shown the 7th harmonic component detection of the load 3 using the both methods. However, it is important to remind now that it is 7th harmonic component multiple of 61Hz. The DFT window is still set for the 60hz component and its multiples.

As a result, there is a lag in its detected harmonic signal. The SOGI-PLL based method adapts dynamically and can tracking the new signal. With this study, it can be concluded that DFT based method is faster and more accurate in the harmonic detection than SOGI-PLL based method, however, it may differ in detection during a fluctuation of the grid voltage frequency. The dynamic error of both methods in the harmonic detection during this study are shown in Fig. 10.

IV. CASE STUDY

In this section, a case study is performed comparing the selective harmonic current compensation using the harmonic current detection strategies SOGI-PLL and DFT. These methods are applied in a three-phase grid-connected photovoltaic system. In this way, if the power generation of the photovoltaic system is below its nominal, this system can be used for harmonic current compensation of nonlinear loads connected at the point of common coupling. The nominal power of the system is 5kW.

It is used a solar array with 1 strings composed of 20 modules of 250 W in series connection. The simulation was implemented in PLECS and Matlab environments.
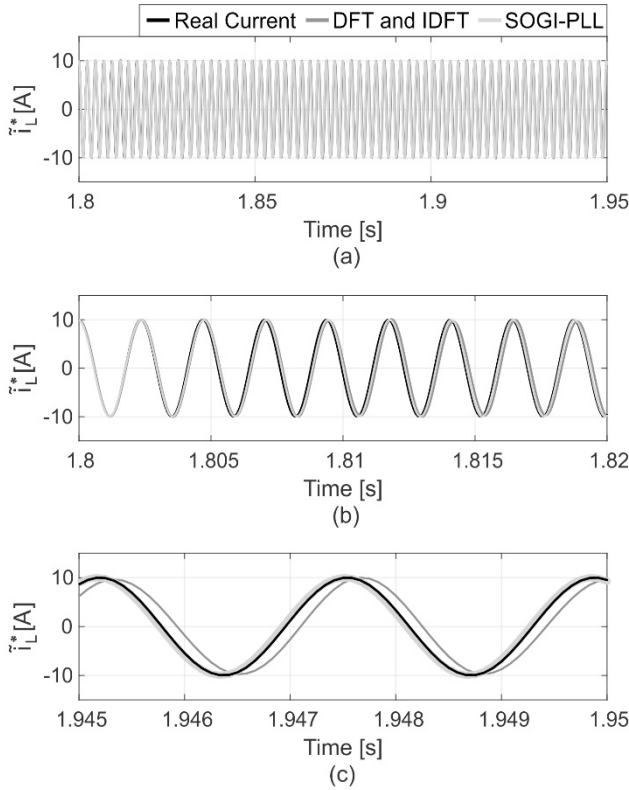
Fig. 9. The 7th harmonic component detection of the load 3. (a) General overview. (b) Transient response. (c) Steady state response.
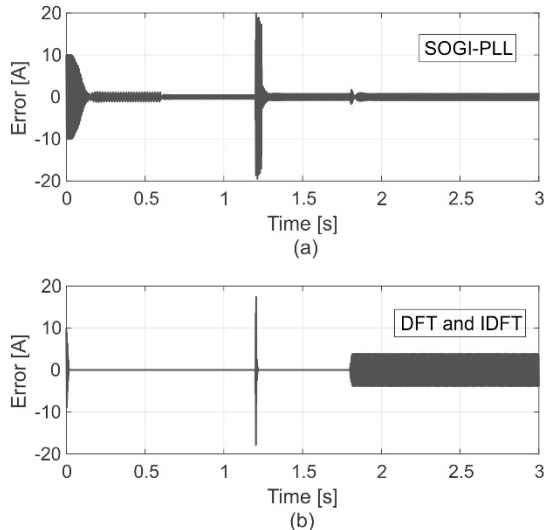
Fig. 10. The dynamic error of both methods in the harmonic detection during this study. (a) SOGI-PLL based method error. (b) DFT and IDFT based method error.

The photovoltaic inverter control strategy is composed of an outer loop responsible for controlling the dc bus voltage, the controller used in this loop is a proportional-integrator (PI). Furthermore, there is an inner loop responsible for controlling the inverter current, the controller used in this loop is a proportional multi-resonant. It is important to note that the harmonic detector strategies approached in this work are capable to tune, dynamically, the resonant controller, because they also detect the frequency of the harmonic of higher amplitude to be compensated.

The nonlinear loads in this case study are the same shown in Fig. 6. Initially, the spectrum of the load connected in the PCC is represented by the Fig. 6 (a). The harmonic compensation is turned on in 0.6 seconds and the 5th harmonic is detected by both strategies. Fig. 11 shows the grid current. Note a grid current waveform improvement after 0.6 seconds and the faster response of the DFT and IDFT in relation to the SOGI-PLL. In steady state, the SOGI-PLL strategy ensures a grid current THD equal to 43.94% and DFT ensures 43.64%.

In 1.2 seconds, the harmonic current content of the load current changes and now the 7th harmonic has higher amplitude, as shown in Fig. 6 (b). Fig. 12 shows the grid current around of this time. Note over again the faster response of the DFT and IDFT in relation to the SOGI-PLL. In steady state, the SOGI-PLL strategy ensures a grid current THD equal to 44.42% and DFT ensures 43.75%.
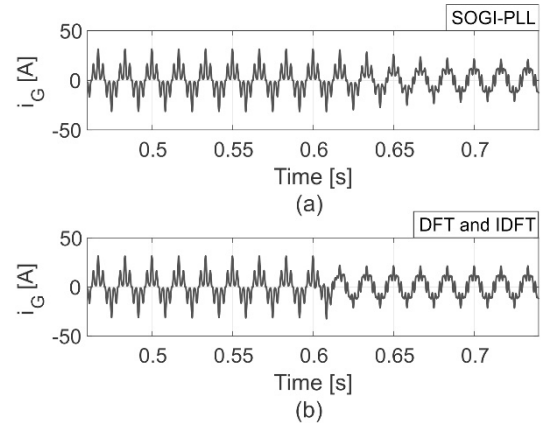
Fig. 11. Grid current waveform details around 0.6 seconds. (a) SOGI-PLL based method. (c) DFT and IDFT based method.

Tabela 1 - Total harmonic distortion of the Grid current.

	SOGI-PLL	DFT and IDFT
t<0.6	87.77%	87.77%
0.6<t<1.2	43.94%	43.64%
1.2 <t<1.8	44.42%	43.75%
t>1.8	44.00%	56.22%
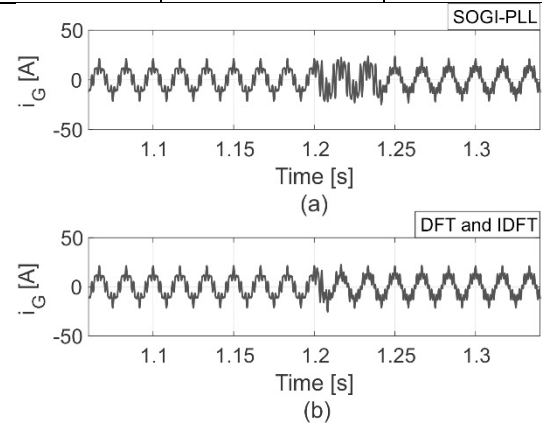
Fig. 12. Grid current waveform details around 1.2 seconds. (a) SOGI-PLL based method. (c) DFT and IDFT based method.

In 1.8 seconds, the fundamental frequency of the grid voltage changes from 60Hz to 61Hz, this fact changes the load current frequency. Fig. 13 shows the grid current around of this time. In this time, note that the error in the detection using the DFT based method causes a worsening in the grid current waveform in relation to the SOGI-PLL based method.
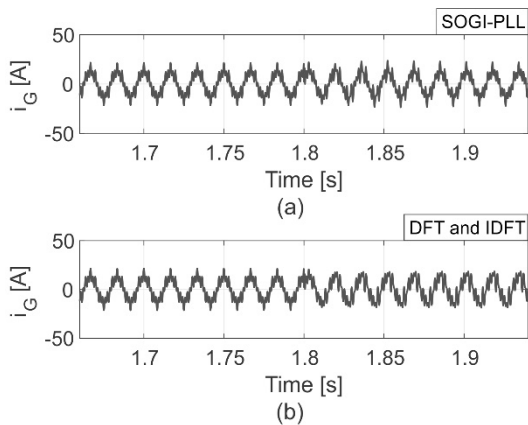
Fig. 13. Grid current waveform details around 1.8 seconds. (a) SOGI-PLL based method. (c) DFT and IDFT based method.

V. CONCLUSIONS

This work presented a comparison between three current harmonic detection methods. Two of them based on the DFT, and one based on the SOGI-PLL method. The method based on DFT are faster and more accurate in the harmonic detection than the SOGI-PLL based method. However, if variations in the grid frequency happened, it may cause problems in the methods based on Fourier transform.

All methods are used in a PV inverter, in order to compensate the load harmonic current, reducing the grid current THD. Partial results showed that DFT methods presented problem to be used in PV inverters during variation in the grid frequency, increasing the grid current distortion.

ACKNOLEDGEMENTS

REFERENCES

[1] D. Yazdani, A. Bakhshai, G. Joos e M. Mojiri, "A Real-Time Three-Phase Selective-Harmonic-Extraction Approach for Grid-Connected Converters," *IEEE Transactions on Industrial Electronics,* vol. 56, nº 10, pp. 4097-4106, 2009.

[2] B. Singh, K. Al-Haddad e A. Chandra, "A review of active filters for power quality improvement," *IEEE Transactions on Industrial Electronics,* vol. 46, nº 5, pp. 960-971, 1999.

[3] S. Rechka, E. Ngandui, J. Xu e P. Sicard, "Analysis of harmonic detection algorithms and their application to active power filters for harmonics compensation and resonance damping," *Canadian Journal of Electrical and Computer Engineering,* vol. 28, nº 1, pp. 41-51, 2003.

[4] D. Tian, Z. Zhu e C. Chen, "A Selective Harmonic Optimization Method for STATCOM in Steady State Based on the Sliding DFT," em *2015 IEEE International Conference on Systems, Man, and Cybernetics*, Kowloon, 2015.

[5] Y. Yu, Y. Xu e X. Liu, "Research of Improved Iterative DFT Method in Harmonic Current Detection," em *2011 Asia-Pacific Power and Energy Engineering Conference*, Wuhan, 2011.

[6] L. S. Xavier, A. F. Cupertino, V. F. Mendes e H. A. Pereira, "A novel adaptive current harmonic control strategy applied in multifunctional single-phase solar inverters," em *2015 IEEE 13th Brazilian Power Electronics Conference and 1st Southern Power Electronics Conference (COBEP/SPEC)*, Fortaleza, 2015.

[7] B. Chen, G. Pin, W. M. Ng, T. Parisini e S. Y. R. Hui, "A Fast-Convergent Modulation Integral Observer for Online Detection of the Fundamental and Harmonics in Grid-Connected Power Electronics Systems," *IEEE Transactions on Power Electronics ,* vol. 32, nº 4, pp. 2596-2607, 2017.

[8] J. Li-jun, C. Yi-fan, Y. Guang-yao, J. Miao-miao, Z. Hai-peng e Z. Ke, "Research on detection and elimination methods of the micro grid harmonics based on the continuous wavelet transform," em *2015 IEEE 10th Conference on Industrial Electronics and Applications (ICIEA)*, Auckland, 2015.

[9] J. R. Vazquez e P. Salmeron, "Active power filter control using neural network technologies," *IEE Proceedings - Electric Power Applications,* vol. 150, nº 2, pp. 139-145, 2003.

[10] L. Yang, C. Xiong, Y. Teng, Q. Hui e Y. Zhu, "Study on Harmonic Current Detection in Grid-Connected PV Generation Systems," em *2015 Sixth International Conference on Intelligent Systems Design and Engineering Applications (ISDEA)*, Guiyang, 2015.

[11] S. K. Jain, P. Agrawal e H. O. Gupta, "Fuzzy logic controlled shunt active power filter for power quality improvement," *IEEE Proceedings - Electric Power Applications,* vol. 149, nº 5, pp. 317-328, 2002.

[12] L. Asiminoaei, F. Blaabjerg e S. Hansen, "Evaluation of harmonic detection methods for active power filter applications," *Twentieth Annual IEEE Applied Power Electronics Conference and Exposition,* vol. 1, pp. 635-641, 2005.

[13] J. Zhan, X. Cheng, Q. Xu, L. Wu e G. Chen, "Design of comprehensive motor protector based on improved sliding window iterative DFT algorithm," *2016 IEEE 8th International Power Electronics and Motion Control Conference (IPEMC-ECCE Asia),* pp. 3658-3662, 2016.

[14] M. Ciobotaru, R. Teodorescu e F. Blaabjerg, "A New Single-Phase PLL Structure Based on Second Order Generalized Integrator," em *IEEE Power Electronics Specialists Conference*, 2006.

[15] R. Teodorescu, M. Liserre e P. Rodriguez, Grid Converters for Photovoltaic and Wind Power Systems, Wiley-IEEE Press, 2011.

[16] S. Golestan e J. M. Guerrero, "Conventional Synchronous Reference Frame Phase-Locked Loop is an Adaptive Complex Filter," *IEEE Trans. Ind. Electron.,* pp. 1679-1682, Mar. 2015.